

Pre-existing immune status associated with response to combination of sipuleucel-T and ipilimumab in patients with metastatic castration-resistant prostate cancer

Meenal Sinha ,¹ Li Zhang,^{1,2} Sumit Subudhi,³ Brandon Chen,¹ Jaqueline Marquez,¹ Eric V Liu,¹ Kate Allaire,¹ Alexander Cheung,¹ Sharon Ng,¹ Christopher Nguyen,¹ Terence W Friedlander,^{1,4} Rahul Aggarwal,^{1,4} Matthew Spitzer,^{5,6} James P Allison,³ Eric J Small,^{1,4} Padmanee Sharma,^{3,7} Lawrence Fong^{1,7}

To cite: Sinha M, Zhang L, Subudhi S, *et al.* Pre-existing immune status associated with response to combination of sipuleucel-T and ipilimumab in patients with metastatic castration-resistant prostate cancer. *Journal for ImmunoTherapy of Cancer* 2021;**9**:e002254. doi:10.1136/jitc-2020-002254

► Additional material is published online only. To view, please visit the journal online (<http://dx.doi.org/10.1136/jitc-2020-002254>).

Accepted 01 April 2021

ABSTRACT

Background Sipuleucel-T is a US Food and Drug Administration-approved autologous cellular immunotherapy that improves survival in patients with metastatic castration-resistant prostate cancer (mCRPC). We examined whether administering ipilimumab after sipuleucel-T could modify immune and/or clinical responses to this treatment.

Methods A total of 50 patients with mCRPC were enrolled into a clinical trial (NCT01804465, ClinicalTrials.gov) where they received ipilimumab either immediately or delayed 3 weeks following completion of sipuleucel-T treatment. Blood was collected at various timepoints of the study. Luminex assay for anti-prostatic acid phosphatase (PAP) and anti-PA2024-specific serum immunoglobulin G (IgG) and ELISpot for interferon- γ (IFN- γ) production against PAP and PA2024 were used to assess antigen-specific B and T cell responses, respectively. Clinical response was defined as >30% reduction in serum prostate-specific antigen levels compared with pretreatment levels. The frequency and state of circulating immune cells were determined by mass cytometry by time-of-flight and statistical scaffold analysis.

Results We found the combination to be well tolerated with no unexpected adverse events occurring. The timing of ipilimumab did not significantly alter the rates of antigen-specific B and T cell responses, the primary endpoint of the clinical trial. Clinical responses were observed in 6 of 50 patients, with 3 having responses lasting longer than 3 months. The timing of ipilimumab did not significantly associate with clinical response or toxicity. The combination treatment did induce CD4 and CD8 T cell activation that was most pronounced with the immediate schedule. Lower frequencies of CTLA-4 positive circulating T cells, even prior to treatment, were associated with better clinical outcomes. Interestingly, these differences in CTLA-4 expression were associated with prior localized radiation therapy (RT) to the prostate or prostatic fossa. Prior radiation treatment was also associated with improved radiographic progression-free survival.

Conclusion Combining CTLA-4 blockade with sipuleucel-T resulted in modest clinical activity. The timing of CTLA-4 blockade following sipuleucel-T did not alter antigen-specific responses. Clinical responses were associated with both lower baseline frequencies of CTLA-4 expressing T cells and a history of RT. Prior cancer therapy may therefore result in long-lasting immune changes that influence responsiveness to immunotherapy with sipuleucel-T and anti-CTLA-4.

INTRODUCTION

Sipuleucel-T is an FDA-approved autologous cellular immunotherapy for the treatment of asymptomatic or minimally symptomatic metastatic castration-resistant prostate cancer (mCRPC).¹ Sipuleucel-T is manufactured by culturing isolated peripheral blood mononuclear cells (PBMCs) with PA2024, a recombinant fusion protein composed of prostatic acid phosphatase (PAP) linked to granulocyte-macrophage colony-stimulating factor (GM-CSF). Sipuleucel-T has been shown to function as a cancer vaccine, priming T and B cell immune responses to PA2024, both of which are associated with improved overall survival (OS).^{1,2} This vaccine has also been shown to recruit T cells to the tumor microenvironment and induce the expression of inhibitory immune checkpoints including CTLA-4.^{3,4} The latter may serve to dampen treatment-induced immune responses.

CTLA-4 blockade with ipilimumab is approved as monotherapy for the treatment of melanoma, and in combination with programmed cell death protein 1 (PD-1) blockade in melanoma, kidney, hepatocellular, and lung cancers. Ipilimumab has been



© Author(s) (or their employer(s)) 2021. Re-use permitted under CC BY-NC. No commercial re-use. See rights and permissions. Published by BMJ.

For numbered affiliations see end of article.

Correspondence to

Dr Lawrence Fong;
lawrence.fong@ucsf.edu

studied in mCRPC in two randomized phase III clinical trials: one in the post-docetaxel setting and one in chemotherapy-naïve setting. Both failed to demonstrate an improvement in median OS compared with placebo.^{5,6} Nevertheless, in the post-docetaxel trial, the survival rates in years 2–5 are superior in the ipilimumab arm, indicating that a small proportion of patients may derive a durable clinical benefit.⁷

We undertook a phase II clinical trial combining ipilimumab with sipuleucel-T in chemotherapy-naïve patients with mCRPC, predicated on the observation that although sipuleucel-T can induce a Th1 immune response within the prostate cancer microenvironment, immunologic checkpoints including CTLA-4 are also induced. The timeline of the immunologic events induced by sipuleucel-T is not well understood, resulting in uncertainty as to the optimal timing of initiation of immune checkpoint inhibition following sipuleucel-T therapy. Consequently, we designed a trial that would begin to address the optimal timing of ipilimumab administration following treatment with sipuleucel-T.

METHODS

Clinical study

A multicenter, open-label phase II clinical trial (NCT01804465) was undertaken that enrolled and followed patients from April 2014 to November 2020. Eligible patients had asymptomatic or minimally symptomatic mCRPC, defined as progressive prostate cancer by PCWG2 criteria in the face of castrate levels of testosterone.⁸ Patients with liver metastases were excluded, as were patients with ECOG performance status of 3 or worse. Adequate end organ function (liver, kidney, hematologic) was required. Androgen deprivation was continued in all patients, and prior chemotherapy for mCRPC was an exclusion criterion. All patients received sipuleucel-T administered in standard fashion (intravenous infusion once every 2 weeks for a total of 3 doses). Patients were subsequently randomized to receive their first dose of ipilimumab either immediately (within minutes) following their last sipuleucel-T infusion (immediate arm), or 3 weeks after their last sipuleucel-T infusion (delayed arm) (Figure S1). After initiating ipilimumab therapy, all patients received an additional 3 doses of ipilimumab, 3mg/kg IV every 3 weeks, for a total of 4 ipilimumab doses given 3 weeks apart. Patients remained enrolled on the clinical trial until disease progression. The study allowed for patients who experienced an initial response, either by radiographic assessment or by at least a 30% reduction in pre-treatment PSA levels in blood, and then subsequently progressed could be reinduced with another 4 cycles of ipilimumab every 3 weeks. The primary endpoint was to determine the impact of timing of ipilimumab treatment on the induction of antibodies to PAP and PA2024 following treatment. Secondary endpoints included efficacy (as measured by the proportion of patients experiencing a >30% decline

in their serum PSA level, duration of PSA decline, radiologic progression-free survival (rPFS) and overall survival, safety as measured by the severity and distribution of adverse events, and other immunomodulatory effects of the treatment. Patients were accrued at The University of California San Francisco (UCSF) and The University of Texas MD Anderson Cancer Center (MDACC). Each patient provided signed informed consent; and relevant institutional review boards approved the study protocols, including the collection of biospecimens.

Antibody response assessment

Immunoglobulin G (IgG) levels against PAP and PA2024, the PAP-GM-CSF fusion protein used to manufacture sipuleucel-T, were evaluated by Life Technologies Corporation using Luminex xMAP technology, which uses multiplexed antigen-coated spectrally distinguishable fluorescence dyed beads. Serum samples (30 µL) were assessed at 1:200 dilution, and normalized signal intensities were log₂-transformed for analysis. Non-specific background signal was measured using bovine serum albumin, glutathione s-transferase (GST) and anti-GST-conjugated beads, and data were normalized based on a linear model to reduce technical variability.⁹ Antibody titers ≥1:400 were considered to be positive.

ELISpot and proliferation assays

Cryopreserved PBMCs were thawed and rested overnight at 37°C for batch analysis. The cells were then plated in triplicate of 3.0×10⁵ cells/well and incubated with recombinant PAP or PA2024 at 25 µg/mL, leucoagglutinin PHA-L at 10 µg/mL (Sigma, Cat # L2769) or without antigen for 48 hours at 37°C in MultiScreen Filter Plates (Millipore, Cat # S2EM004M99). Cells secreting interferon-γ (IFN-γ) were visualized by anti-human-IFN-γ enzyme-linked immunospot assay (ELISpot) (MABTECH, Cat # 3420-2A). Plates were scanned with an automated ELISpot plate reader (CTL-ImmunoSpot Analyzer). Spots were counted using CTL Immunospot V.5.0 analyzer software. Final counts of antigen-specific IFN-γ secreting cells were obtained by subtracting the number of spots counted in no-antigen control wells from test wells. Samples were accepted for inclusion in final analysis if positive control PHA wells had an average >100 spots/well, and negative control (no antigen) wells had <100 spots/well.

For the proliferation assays, the cells were plated in triplicate of 1.0×10⁵ cells/well and incubated with recombinant PAP or PA2024 at 25 µg/mL, leucoagglutinin PHA-L at 3 µg/mL (Sigma, Cat# L2769) or without antigen for 120 hours at 37°C. ³H-thymidine 1 mCi was then added, and the cells were incubated for another 8 hours at 37°C. Cells were harvested and assessed on a Perkin Elmer MicroBeta Trilux.

Mass cytometry staining and analysis

Available cryopreserved PBMC samples were thawed, barcoded, and stained with heavy metal-labeled antibodies for analysis by mass cytometry by time-of-flight

(CyTOF). These samples were then washed and acquired on a mass cytometer (Helios, Fluidigm). Contour plot data were generated for CD3+ T cells with Cytobank.¹⁰ We used *flowCore* V.2.0.1 (<https://rdrr.io/bioc/flowCore/>) to load the data into R V.4.0.2, *uwot* (<https://arxiv.org/abs/1802.03426>) to make the UMAP projection, *Rphenograph*¹¹ for clustering, and *ggplot2* (<https://ggplot2.tidyverse.org>) for plotting. The calculation of both the UMAP projection and the clustering was based on the relative staining levels of CD3, CD4, CD8a, CD11b, CD11c, CD14, CD16, CD19, CD25, CD31, CD33, CD45RA, CD56, CD66, CD117, CD123, CD127, CD235ab/CD61, BDCA3, CCR7, FcεR1a, FoxP3, γδTCR, HLA-DR, T-bet, TCR Va24-Ja18, and VISTA. Rphenograph clustering with a *k* value of 200 yielded eight clusters, which were annotated based on the relative staining levels of CD4, CD8, FoxP3, CD25, CD127, CCR7, CD45RA, T-bet, and HLA-DR. For clarity of visualization, the expression values of Ki-67 were capped at the 99th quantile. Cytobank was used to perform manual gating and to create landmark nodes for statistical scaffold analysis.¹² Live T cells (Singlets, Intercalator+, Cisplatin-, CD45+, CD61-, CD235ab-, CD19-, CD3+) were extracted from the fcs files and divided into 30 unsupervised clusters using statistical scaffold. Clusters were assigned vectors associated with the average median value of markers and edges, which are defined as similarity between vectors to produce graphs, which show the relationships between different clusters. Cluster frequencies and Boolean expression for functional markers for each cluster were passed through the Significance Across Microarrays algorithm and results were formulated into the scaffold maps for visualization (github.com/nolanlab/scaffold). For scaffold heatmaps, fold change, significance, cell count, and nearest landmark node, data were extracted from the outputs of the scaffold analysis using a custom script. The heatmap was created in R using *pheatmap* (<https://CRAN.R-project.org/package=pheatmap>), with \log_2 fold change capped at 2.

Statistical considerations and analysis

This is a multicenter non-comparative randomized phase II trial with the primary objective of immunologic efficacy in addition to safety. Immune response was defined as an IgG antibody response to either PAP or PA2024 by study week 20. The IgG antibody response was determined by ELISA with a positive response defined as titer $\geq 1:400$. To achieve a 40% immune response rate indicating immune activity versus a null hypothesis of 15% indicating lack of immune activity assuming a two-sided type I error of 5% and 81% power would require 27 total patients per arm, based on the exact binomial test. Patients were accrued at UCSF and MDACC with the randomization to ipilimumab timing stratified by institution.

Baseline characteristics were summarized as frequencies and percentages or medians and ranges. Comparison of the categorical and continuous variables between two arms was performed by χ^2 test and Wilcoxon rank-sum test, respectively. rPFS was analyzed using the Kaplan-Meier

method and compared between arms using the unstratified log-rank test and Cox proportional hazards regression model. Time to radiographic progression was defined as the time from randomization to the date of documented radiographic progression or last available follow-up date. OS was defined as the time from randomization to the date of death or last available follow-up date. Changes in PSA and immune response parameters within each arm were evaluated using a non-parametric Wilcoxon signed-rank test. A clinical response was defined as at least 30% reduction in serum PSA level at any time during treatment compared with pretreatment value for that patient. Analogously, changes in PSA and immune response parameters between arms were evaluated using a non-parametric Wilcoxon rank-sum test. All reported *p* values are two-sided, and $p < 0.05$ was used to define statistical significance.

RESULTS

Clinical outcomes

Fifty patients were randomized, with 26 allocated to the delayed ipilimumab arm and 24 to the immediate ipilimumab arm as in the study design (online supplemental figure 1). Patient disposition is summarized in online supplemental figure 2. The baseline clinical characteristics of patients were similar between the arms (table 1). Overall, 5 of 50 patients (10%) had >50% decline in their serum PSA level, and 1 additional patient had a PSA decline >30% but <50%. The duration of PSA decline of >50% to PSA progression in the five responding patients was 55, 84, 140, 435 and 689 days (figure 1A). These responses were distributed between the treatment arms (figure 1B). The rPFS for the entire group was 5.72 months (95% CI 3.95 to 6.58) (figure 1C), and rPFS was similar between the two arms (figure 1D). The median OS was 31.9 months (95% CI 27.2 to 43.7) (figure 1E), with no significant difference between the arms (figure 1F). In univariate analyses, baseline PSA, baseline hemoglobin and prior radiation therapy (RT) were associated with rPFS (online supplemental table 1). Multivariate analyses did not reveal any significant findings.

The treatment was well tolerated, and immune-related adverse events (irAEs) were consistent with prior reports of irAEs with ipilimumab. There was a single grade 4 event consisting of colitis with colonic perforation requiring surgery and a total of nine grade 3 events in seven patients (table 2). There was no difference in frequency or distribution of irAEs between the two treatment arms. Patients with an irAE were more likely to have a PSA response (any grade, $p=0.001$, grade 3/4, $p=0.037$).

Modulation of antigen-specific immune responses

Antigen-specific IgG antibody responses and ELISpot responses to PA2024 were associated with improved survival with sipuleucel-T.^{1 13} In this trial, the primary endpoint was to determine the proportion of patients in each study arm who achieved an antibody titer of $\geq 1:400$

Table 1 Baseline patient demographics

		Overall	Delayed ipilimumab arm	Immediate ipilimumab arm	p value
<i>n</i>		50	26	24	
Age	(Median (range))	67.50 (51.00, 79.00)	67.00 (57.00, 77.00)	68.00 (51.00, 79.00)	0.961
Race (%)	Asian	3 (6.8)	1 (4.3)	2 (9.5)	0.607
	Black or African-American	3 (6.8)	1 (4.3)	2 (9.5)	
	White	38 (86.4)	21 (91.3)	17 (81.0)	
	NA	6 (12.0)	3 (11.5)	3 (12.5)	
Ethnicity (%)	Hispanic or Latino	4 (10.0)	2 (9.5)	2 (10.5)	1
	Non-Hispanic	36 (90.0)	19 (90.5)	17 (89.5)	
	NA	10 (20.0)	5 (19.2)	5 (20.8)	
Gleason score at diagnosis (%)	7	19 (38.8)	8 (30.8)	11 (47.8)	0.353
	>7	30 (61.2)	18 (69.2)	12 (52.2)	
	NA	1 (2.0)	0 (0.0)	1 (4.2)	
ECOG Performance	0	42 (84.0)	24 (92.3)	18 (75.0)	0.2
	1	8 (16.0)	2 (7.7)	6 (25.0)	
Status (%)					
Site of disease (%)	Lymph node only	8 (16.0)	5 (19.2)	3 (12.5)	0.673
	Bone with or without lymph node	37 (74.0)	20 (76.9)	17 (70.8)	
	Any visceral	5 (10.0)	1 (3.8)	4 (19.0)	
Prior treatment (%)	Radical prostatectomy	6 (12.0)	3 (11.5)	3 (12.5)	0.848
	Radiation therapy	14 (28.0)	8 (30.8)	6 (25.0)	
	Both	20 (40.0)	11 (42.3)	9 (37.5)	
	Neither	10 (20.0)	4 (15.4)	6 (25.0)	
PSA	(Median (range))	6.26 (0.10, 311.60)	8.62 (0.25, 83.74)	5.68 (0.10, 311.60)	0.485
Alkaline phosphatase	(Median (range))	81.50 (37.00, 257.00)	83.00 (37.00, 173.00)	80.50 (39.00, 257.00)	0.963
Lactate dehydrogenase	(Median (range))	136.00 (56.00, 402.00)	83.50 (56.00, 111.00)	172.00 (109.00, 402.00)	0.121
Hemoglobin	(Median (range))	12.80 (10.90, 14.60)	12.80 (11.30, 14.60)	12.90 (10.90, 14.50)	0.394

PSA, prostate-specific antigen .

to PA2024 and/or PAP following treatment. Overall, the majority of the patients (78.6%) had induced antibodies post-treatment above this titer. There was no significant difference between the two arms (71.4% for the immediate arm and 81% for the delayed arm, $p=1$). T cell immune responses were evaluated by assessing proliferative responses of PBMC to antigen. Therapy with the combination of sipuleucel-T and ipilimumab induced significant proliferation to PA2024 and PAP, which were detectable at multiple timepoints (figure 2A,B), with no significant difference between arms (online supplemental figure 3). Immune responses assessed by IFN- γ ELISpot also identified the induction of T cell responses to PA2024 and PAP (figure 2C,D), although these responses

were less durable than the proliferative responses. There were again no differences between arms (online supplemental figure 3). RT prior to immunotherapy did not significantly affect any of the antigen-specific immune responses either before or at any timepoint after immunotherapy treatment.

Circulating T cell proliferation and activation

High-dimensional mass cytometry (CyTOF) was used to more broadly determine the effects of immunotherapy in the circulating T cell compartments (figure 3A, left panel). Consistent with our prior observations,¹⁴ we found that ipilimumab treatment induced Ki-67 expression in both CD4 and CD8 T cells (figure 3A, right panel).

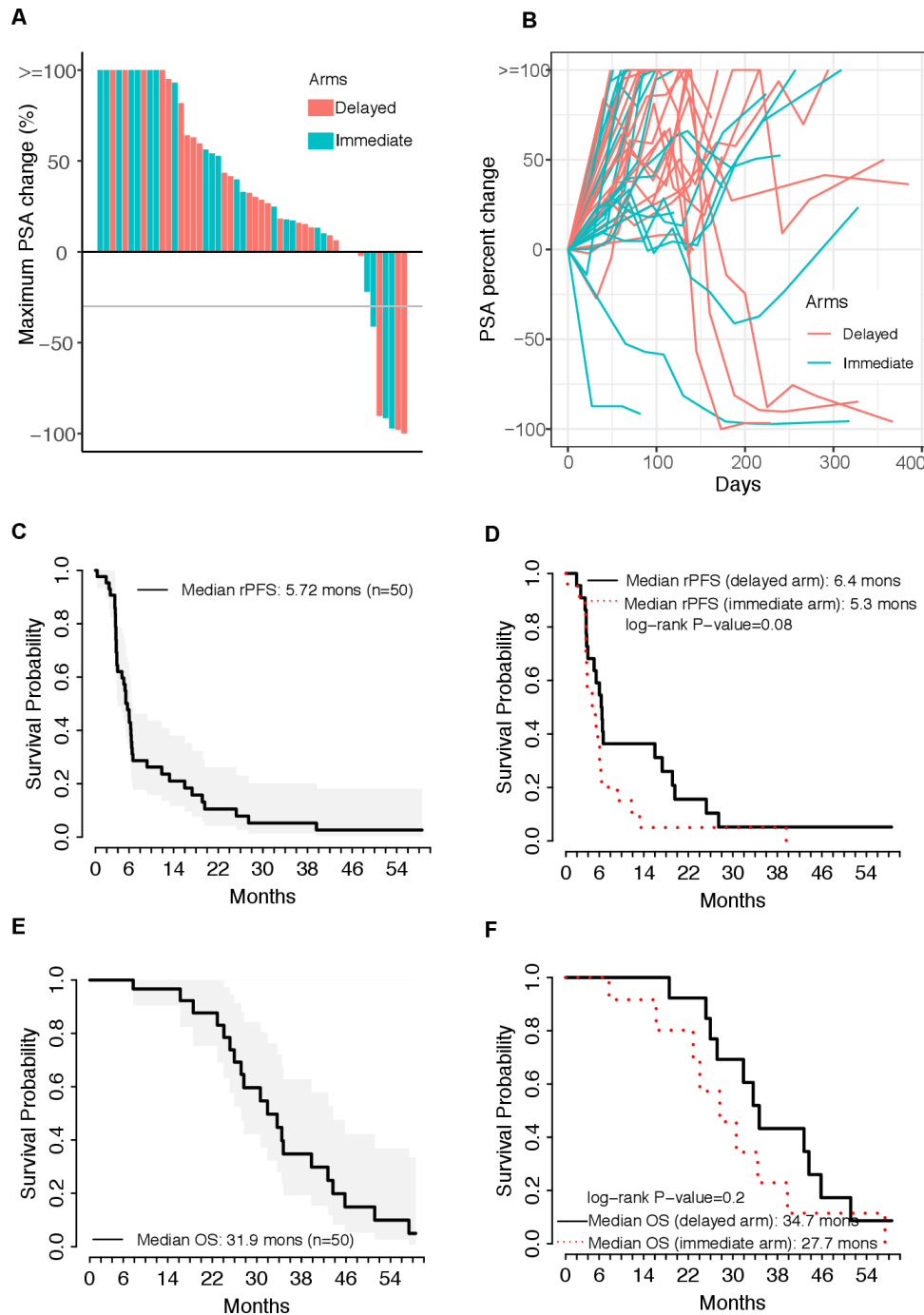


Figure 1 Clinical outcomes. (A) Prostate-specific antigen (PSA) waterfall plot showing the maximal percent change in PSA compared with baseline. (B) Spider plot of PSA at baseline and subsequent changes compared with baseline. (C) Kaplan-Meier plot of time to radiographic progression. Time to radiographic progression was defined as the time from randomization to the date of documented radiographic progression or last available follow-up date. (D) Kaplan-Meier plots of time to radiographic progression separated by treatment cohort. (E) Kaplan-Meier plot of overall survival (OS). OS was defined as the time from randomization to the date of death or last available follow-up date. (F) Kaplan-Meier plots of OS separated by treatment cohort. Comparisons made by log-rank test, with $p < 0.05$ considered statistically significant. rPFS, radiographic progression-free survival.

This induction was most pronounced at timepoint (TP) 3 with immediate arm and at TP4 with the delayed arm (figure 3A, right panel). To assess the changes in the activation state of the different T cell subtypes, we applied statistical scaffold analysis for the percentage of T cells that were positive for various markers that characterize

the functional state of the T cells. When compared with the pretreatment baseline (TP1), T cells across various subtypes showed Ki-67 induction at both TP3 and TP4 in the immediate arm, but only at TP4 in the delayed arm (figure 3B). In the immediate arm, intense proliferation was induced across all T cell subtype clusters, except in

Table 2 Immune-related adverse events

	Delayed ipilimumab arm (n=26)					Immediate ipilimumab arm (n=24)		
	Grade 1	Grade 2	Grade 3	Grade 4	Total	Grade 2	Grade 3	Total
Adrenal insufficiency	1 (3.8%)	1 (3.8%)	1 (3.8%)	0	3 (11.5%)	1 (4.2%)	0	1 (4.2%)
Diarrhea	2 (7.7%)	0	3 (11.5%)	1 (3.8%)	6 (23.1%)	2 (8.3%)	1 (4.2%)	3 (12.5%)
Hyperthyroidism	2 (7.7%)	1 (3.8%)	0	0	3 (11.5%)	0	0	0
Hypothyroidism	1 (3.8%)	0	0	0	1 (3.8%)	1 (4.2%)	0	1 (4.2%)
Lipase increased	0	0	1 (3.8%)	0	1 (3.8%)	0	2 (8.3%)	2 (8.3%)
Rash	1 (3.8%)	1 (3.8%)	0	0	2 (7.7%)	2 (8.3%)	1 (4.2%)	3 (12.5%)
No of patients (%)	7 (26.9%)	2 (7.7%)	3 (11.5%)	1 (3.8%)	13 (50%)	5 (20.8%)	3 (12.5%)	8 (33.3%)

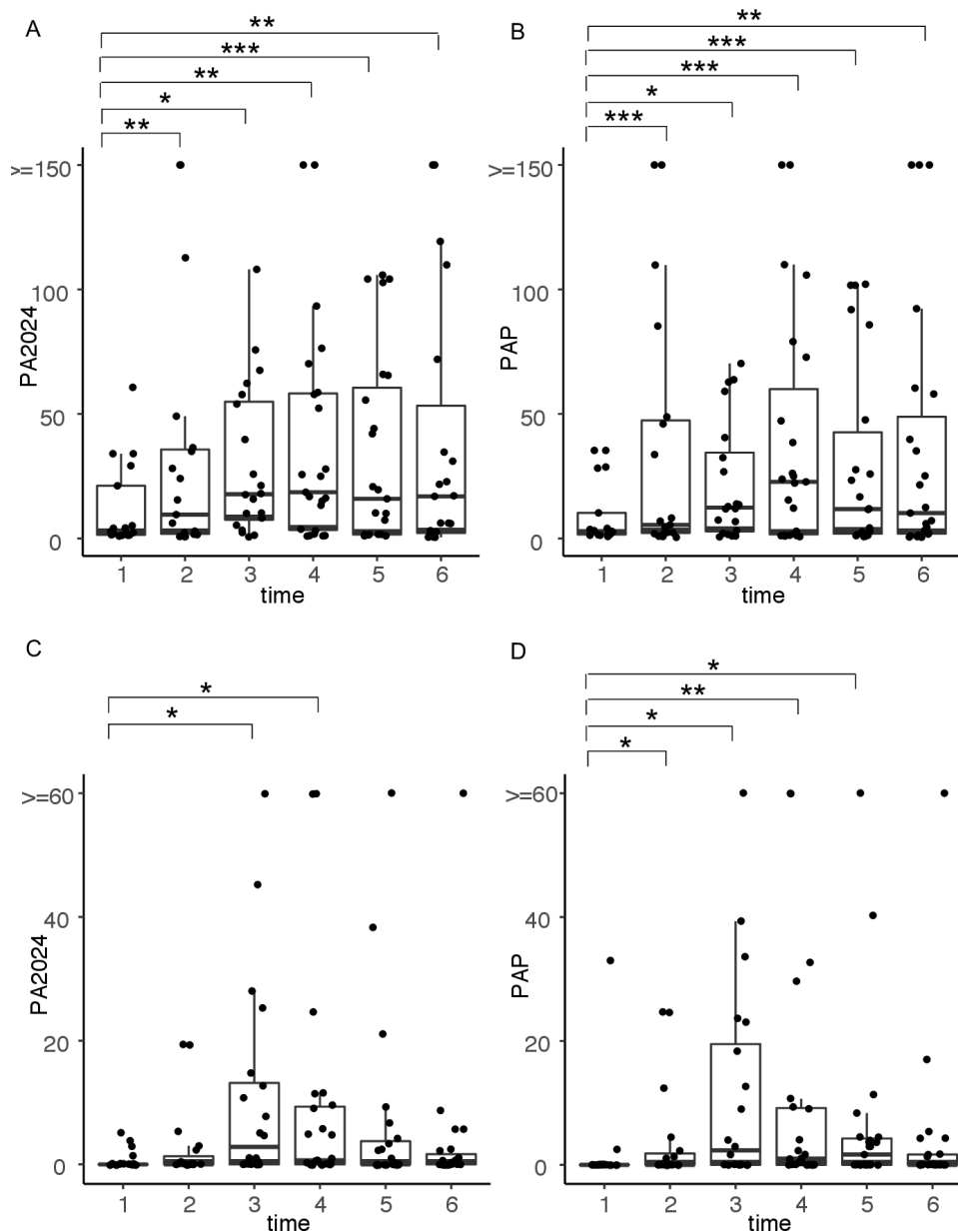


Figure 2 Antigen-specific immune responses over time. T cell proliferation responses to (A) PA2024 and (B) prostatic acid phosphatase (PAP) as measured by ³H-thymidine incorporation are shown across timepoints. Interferon- γ (IFN- γ) T cell immune responses to (C) PA2024 and (D) PAP as measured by ELISpot are shown across timepoints. * p <0.05; ** p <0.01; *** p <0.005.

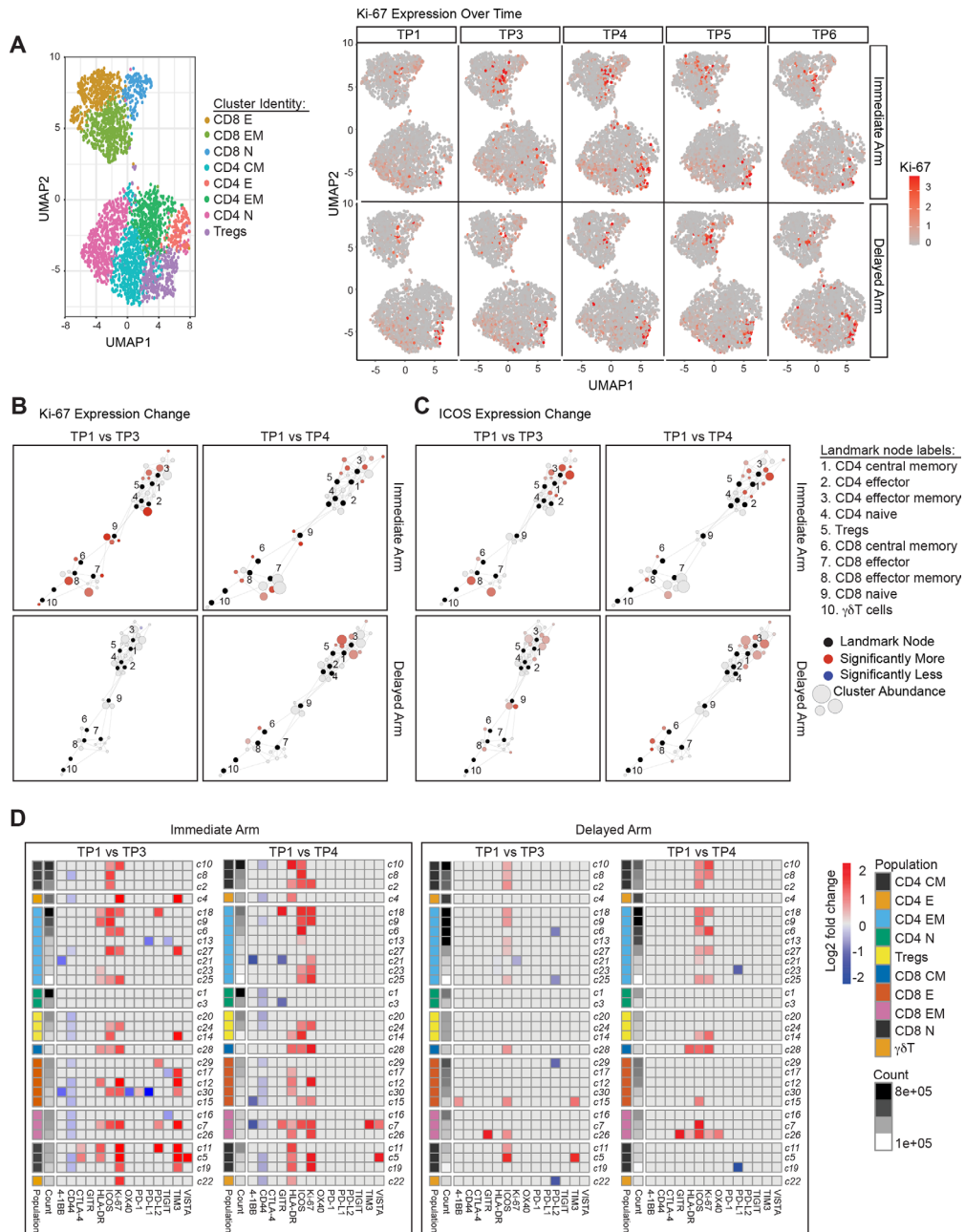


Figure 3 Systemic immune modulation with combination immunotherapy treatment. (A) On the left, a uniform manifold approximation and projection (UMAP) plot of CD3+ T cells from all assessed peripheral blood mononuclear cell (PBMC) samples is shown. Clusters corresponding to canonical T cell subsets are represented using distinct colors. On the right, relative intensity of Ki-67 expression over time is shown for both the immediate and delayed arms of the clinical study. Scaffold maps of significant changes in the percent of Ki-67 (B) or inducible costimulator (ICOS) (C) positive T cell clusters are shown. Clusters are shown when comparing timepoint (TP) 3 or TP4 with pretreatment timepoint TP1 in the immediate and delayed arms of the study. Black-colored nodes in the scaffold maps represent landmark nodes that are canonical T cell types identified by traditional manual cellular gating. The remaining nodes represent the 30 unsupervised T cell clusters created by scaffold analysis. These are arranged around the landmark nodes and each other based on similarity and connected by edges, the length of which is dependent on cluster similarity. The size of the clusters is proportional to cellular abundance. The color coding represents clusters that exhibited significant differences ($q < 0.05$; red=increase, blue=decrease) in percent marker-positive clusters when comparing different two groups. (D) Heatmaps summarizing \log_2 fold changes resulting from statistical scaffold analysis of functional markers 4-1BB, CD44, CTLA-4, GTR, HLA-DR, ICOS, Ki-67, OX40, PD-1, PD-L1, PD-L2, TIGIT, TIM3 and VISTA when comparing pretreatment timepoint TP1 with TP3 and also with TP4 are shown for the immediate and delayed arms. Each box in the heatmap represents a T cell cluster, which has been labeled according to the nearest landmark node that they connect to on a scaffold map and ordered by cell population abundance. The color coding represents clusters that showed a significant difference ($q < 0.05$) in the \log_2 fold change, with red being significantly higher, while blue being significantly lower in group 2 of the two comparison groups. The intensity of the color code is proportional to the \log_2 fold change and is capped at 2 and -2.

CD4-naïve cells, while in the delayed arm, proliferation was observed primarily in the memory CD4 and CD8 T cell compartments at TP4. Consistent with previous studies demonstrating increased expression of inducible costimulator (ICOS) on circulating T cells as a pharmacodynamic biomarker of anti-CTLA-4 therapy,^{15 16} induction of ICOS was also seen on T cells in our current study, primarily on CD4 and CD8 memory T cell subtype clusters (figure 3C). Similar to Ki-67, ICOS induction was observed at both TP3 and TP4 in the immediate arm but was more pronounced at TP4 in the delayed arm (figure 3C). These ICOS findings were confirmed via manual cellular gating using Cytobank (online supplemental figure 4).

To comprehensively assess all T cell activation markers across all of the T cell subtype clusters, we summarized the significant changes, shown as log₂ fold changes, with heatmaps indicating increases in red and reductions in blue, capped at +2 to -2, respectively (figure 3D). Interestingly, the immediate arm, but not the delayed arm, also showed higher levels of HLA-DR expressing T cells across various T cell subtypes when comparing TP1 with TP3 or TP4. The immediate arm also showed higher levels of TIM3 positive cells at TP3 compared with TP1. Taken together, both arms showed increased T cell activation and proliferation after ipilimumab treatment. However, the immediate arm appeared to induce broader and more intense activation across the T cell subtypes.

T cell states differ in clinical responders versus non-responders

To determine whether there were any global differences between PSA clinical responders (\geq PSA30 response) when compared with non-responders, we performed statistical scaffold analysis aggregating all timepoints together and summarized the results in a scaffold heatmap (figure 4). Strikingly, responders showed significantly lower frequency of CTLA-4+ T cells than non-responders when analyzing broadly across all timepoints in both study arms (figure 4A, left panel). When we looked at the different timepoints, this difference was even evident at TP1, which is prior to start of immunotherapy (figure 4A, right panel). Responders also showed higher percentages of T cells positive for ICOS and PD-1 prior to immunotherapy initiation (figure 4B). Flow cytometry plots of CTLA-4 expression on CD3+ T cells confirmed this difference. Taken together, these data suggest that clinical responses defined by PSA declines were associated with lower levels of CTLA-4 positive T cells prior to start of therapy, indicating its potential value as a predictive biomarker for response in this setting. In addition, these responses were also more broadly associated with higher activation and proliferation in T cells (figure 4A, left panel).

In addition, we also assessed if there was a correlation between the durability of the clinical response and the functional state of the T cell populations prior to start of immunotherapy. While these analyses are limited by the small number of responders, we found that patients with a

clinical response lasting \geq 3 months had a lower frequency of CTLA-4+ CD4T cells prior to start of immunotherapy treatment (online supplemental figure 5).

T cell states differ in patients with prior RT versus in those without

Because RT has been shown to be immunomodulatory, we examined whether prior RT as primary treatment to the prostate, as salvage treatment to the prostatic fossa following radical prostatectomy, or as palliative treatment to sites of metastasis, was associated with a difference in the functional states of the T cells. Patients who received prior RT to the prostate received definitive RT with either >66 Gy by external beam or with brachytherapy in combination with external beam radiation.

We found that prior RT was indeed significantly associated with lower frequencies of CTLA-4 positive T cells (figure 5A). Moreover, prior RT was also associated with increased levels of activating molecules 4-1BB and OX40 in CD4, Treg, and CD8 T cell populations. Prior RT was also associated with increased levels of immune checkpoints PD-1 on CD4 T cells and VISTA on both CD4 and CD8 T cells. These differences were apparent on scaffold maps (figure 5B) and on contour plots from Cytobank (figure 5C). Prior RT was also associated with improved rPFS (figure 5D). The Gleason scores for patients that received prior RT versus those that did not were not significantly different ($p=0.972$).

DISCUSSION

Despite significant advances in immunotherapy in multiple cancer types, sipuleucel-T represents the primary approved immunotherapy for prostate cancer. The treatment serves as a vaccine, with the capacity to induce immune responses to a range of antigens. These data support the argument that a fundamental immune defect in prostate cancer is the lack of antigen priming, which can be overcome by sipuleucel-T. Nevertheless, the clinical benefit from sipuleucel-T is modest, indicating that other mechanisms of resistance may be operative. While sipuleucel-T can induce a Th1 immune response within the prostate tumor microenvironment, immunologic checkpoints are also induced including CTLA-4 and TIGIT, but not PD-L1 or VISTA.^{3 4} For this reason, testing the combination of sipuleucel-T together with CTLA-4 inhibition with ipilimumab was reasonable, but disappointingly, failed to provide an obvious improvement over monotherapy with ipilimumab alone.¹⁷ These results do not rule out the possibility that different sequencing of these agents might be beneficial. For example, we did not examine concurrent treatment or pretreatment with ipilimumab prior to sipuleucel-T. It is possible that the capacity of CTLA-4 blockade to induce clonal diversification of the T cell repertoire could actually be beneficial prior to generating sipuleucel-T.¹⁸

In this trial, we also examined whether combining sipuleucel-T and ipilimumab can lead to enhanced immune

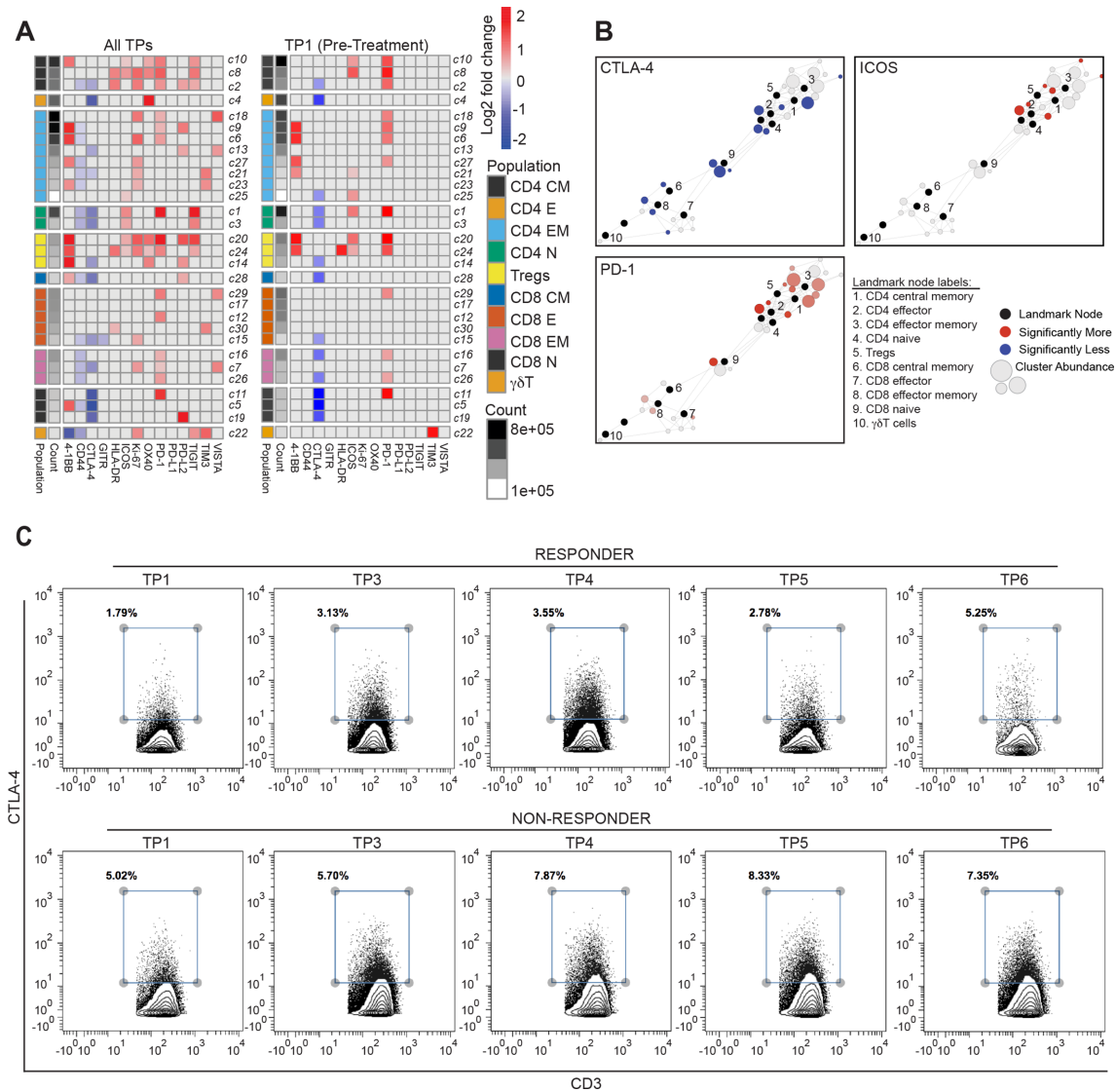


Figure 4 T cell functional states differ in clinical responders compared with non-responders. (A) Heatmaps summarizing \log_2 fold changes resulting from statistical scaffold analysis of functional markers 4-1BB, CD44, CTLA-4, GTR, HLA-DR, ICOS, Ki-67, OX40, PD-1, PD-L1, PD-L2, TIGIT, TIM3 and VISTA are shown for all timepoints (TPs) combined (left panel) and only at pretreatment TP1 (right panel) when comparing responders with non-responders as defined by PSA30 responses. Each box in the heatmap represents a T cell cluster, which has been labeled according to the nearest landmark node that they connect to on a scaffold map and ordered by cell count abundance. The color coding represents clusters that showed a significant difference ($q < 0.05$) in the \log_2 fold change, with red being significantly higher, while blue being significantly lower in group 2 of the two comparison groups. The intensity of the color code is proportional to the \log_2 fold change and is capped at 2 and -2. (B) Scaffold maps for significant changes in CTLA-4, inducible costimulator (ICOS) and PD-1 are shown when comparing non-responders with responders across the entire study at pretreatment TP1. (C) Contour plots from Cytobank manual gating analysis show the percent CTLA-4+ T cells (gated on all CD3+) in a responder (top row) and a non-responder (bottom row) across the various TPs in the study.

responses depending on the scheduling of the dose. We did not see any significant difference in modulating antigen-specific B or T cell immune responses between the immediate and delayed ipilimumab arms. However, some differences in immune activation patterns were observed between the treatment arms: the immediate arm had more dramatic T cell activation with Ki-67 and TIM-3 coexpression, although TIM-3 expression could also serve to blunt immune responses. Despite this difference in T cell activation, we did not see any difference

in clinical activity or toxicities between the arms. Twelve per cent (6/50) of patients had PSA declines $>30\%$, which were evenly distributed between the two arms. PSA decline duration among these patients ranged from 2 to 23 months with three responses ongoing.

One of the most intriguing findings was the association between fewer CTLA-4 positive T cells in the peripheral blood and the PSA responses observed. By using high-dimensional mass cytometry, we found that this association was evident even at the pretreatment timepoint,

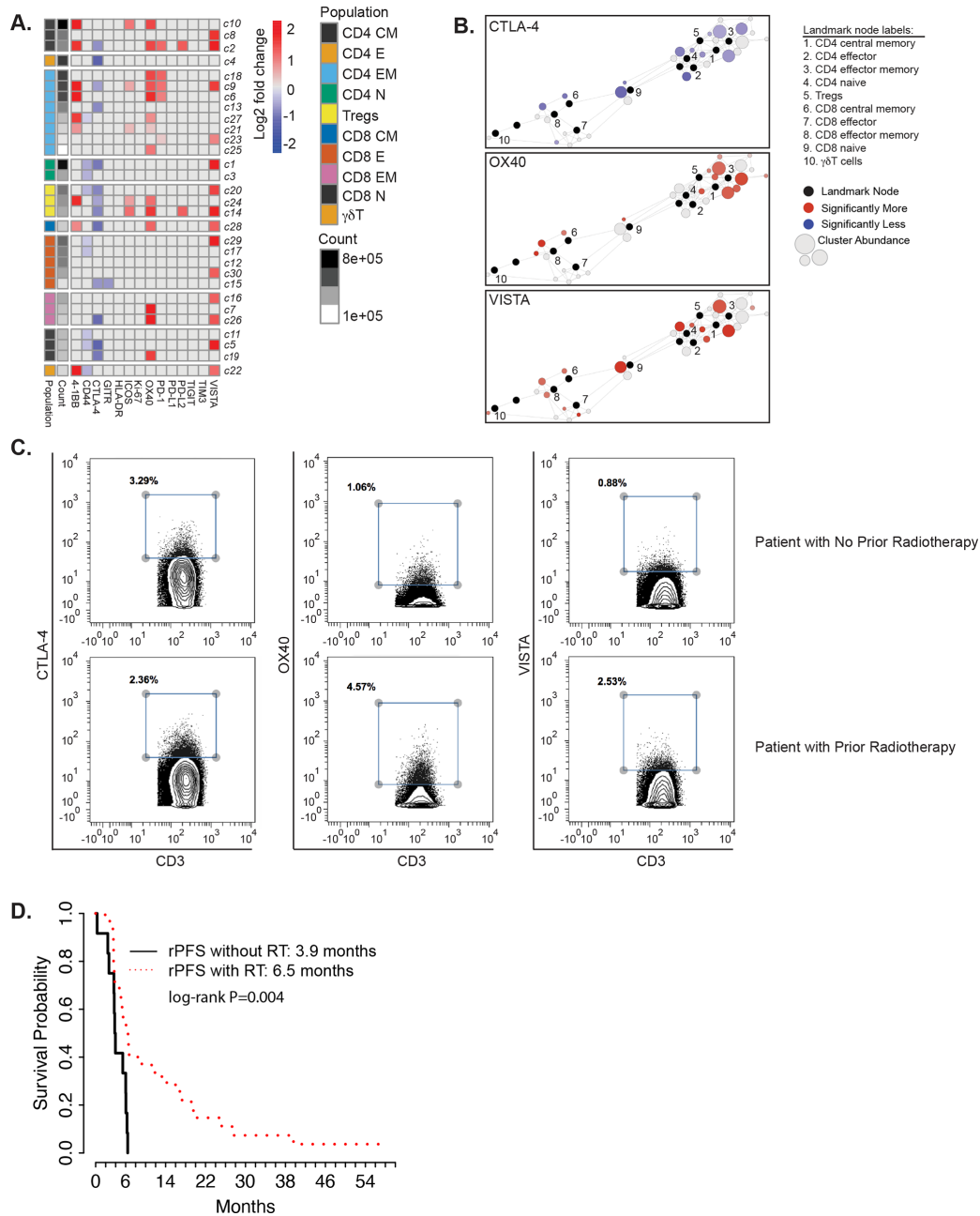


Figure 5 Altered T cell functional states in patients with or without prior radiation therapy (RT). (A) Heatmaps summarizing \log_2 fold changes resulting from statistical scaffold analysis of functional markers 4-1BB, CD44, CTLA-4, GITR, HLA-DR, ICOS, Ki-67, OX40, PD-1, PD-L1, PD-L2, TIGIT, TIM3 and VISTA are shown for the pretreatment timepoint when comparing patients that did not receive radiotherapy to patients that did. Each box in the heatmap represents a T cell cluster, which has been labeled according to the nearest landmark node that they connect to on a scaffold map and ordered by cell count abundance. The color coding represents clusters that showed a significant difference ($q < 0.05$) in the \log_2 fold change, with red being significantly higher, while blue being significantly lower in the RT-treated patients versus patients who did not receive RT. The intensity of the color code is proportional to the \log_2 fold change and is capped at 2 and -2. (B) Scaffold maps for significant changes in CTLA-4, OX40 and VISTA are shown when comparing patients without prior radiotherapy to those with prior radiotherapy across the entire study at pretreatment timepoint. Black-colored nodes in the scaffold maps represent landmark nodes that are canonical T cell types identified by traditional manual cellular gating. The remaining nodes represent the 30 unsupervised T cell clusters created by scaffold analysis. These are arranged around the landmark nodes and each other based on similarity and connected by edges, the length of which is dependent on cluster similarity. The size of the clusters is proportional to cellular abundance. The color coding represents clusters that exhibited significant differences ($q < 0.05$; red=increase, blue=decrease) in percent marker-positive clusters when comparing different two groups. The color intensity is proportional to the \log_2 fold change in the scaffold analysis. (C) Contour plots from Cytobank manual gating analysis showing the percent CTLA-4+, OX40+ and VISTA+ T cells (gated on all CD3+) in a patient with no prior radiotherapy (top row) and a patient with prior radiotherapy (bottom row) at TP1. (D) Kaplan-Meier plots of time to radiographic progression separated by treatment cohort. Comparisons are made by log-rank test, with $*p < 0.05$ considered statistically significant. rPFS, radiographic progression-free survival.

particularly in the naïve CD4 and CD8 T cell compartments. CTLA-4 expression in T cells could potentially serve as a biomarker to allow selection of patients more likely to benefit from this therapy, an observation requiring validation in future trials. This finding also suggests that these patients have some intrinsic differences in their endogenous T cells. This association could represent differences in immunogenicity and/or antigen exposure. Supporting this notion, lower frequencies of CTLA-4 positive T cells were associated with prior RT. Interestingly, a higher frequency of conventional CD4 T cells from RT-treated patients expressed agonist molecules 4-1BB and OX40 as well as immune checkpoints VISTA and PD-1. Regulatory CD4+ T cells from RT-treated patients had higher frequencies of 4-1BB, OX-40, ICOS, and VISTA positivity. Naïve and effector memory CD8 T cells from RT-treated patients also had higher levels of OX-40 and VISTA. Of note, the RT would have been delivered years prior to participation in this study. While the actual mechanism by which prior RT could lead to these durable changes is unknown, RT could lead to enhanced priming and an altered state of immune activation. Because prostate cancer has a predilection for metastasis to bone, obtaining tumor biopsies is challenging in mCRPC. As such, this was not integrated into the clinical trial and we do not have an assessment of the tumor immune microenvironment.

RT has been shown to potentially synergize with immunotherapy in preclinical models.^{19, 20} Clinical responses combining RT with CTLA-4 blockade have also been seen in patients with cancer.^{21, 22} While the phase III clinical trial combining ipilimumab with RT failed to show improved median survival in patients, long-term follow-up demonstrated superior OS in the ipilimumab-treated arm.⁷ This trial irradiated a bone metastasis with a single fraction of RT at the start of ipilimumab and also included only patients who had received prior docetaxel chemotherapy.

In summary, these results demonstrate the importance of prior cancer treatments on impacting response to cancer immunotherapy in these patients with prostate cancer. While administration of sipuleucel-T did not significantly alter the outcome of clinical responses to ipilimumab, prior RT appears to leave not only a lasting impression on the T cell compartment, but also can associate with improved clinical outcomes with immunotherapies. Future studies can help to elucidate the mechanisms that lead to the altered T cell states in patients with advanced cancer and perhaps lead to improved clinical outcomes.

Author affiliations

¹Department Hematology/Oncology, School of Medicine, University of California San Francisco, San Francisco, California, USA

²Department of Epidemiology and Biostatistics, School of Medicine, University of California San Francisco, San Francisco, California, USA

³Department of Genitourinary Medical Oncology, Division of Cancer Medicine, The University of Texas MD Anderson Cancer Center Division of Cancer Medicine, Houston, Texas, USA

⁴Helen Diller Family Comprehensive Cancer Center, University of California San Francisco, San Francisco, California, USA

⁵Department of Otolaryngology-Head and Neck Surgery, University of California San Francisco, San Francisco, California, USA

⁶Department of Microbiology and Immunology, University of California San Francisco, San Francisco, CA, USA

⁷Parker Institute of Cancer Immunotherapy, San Francisco, CA, USA

Twitter Matthew Spitzer @SpitzerLab and Lawrence Fong @lawfong

Acknowledgements We thank Stanley Tamaki, Claudia Bispo and Michael Lee at the UCSF Parnassus Flow Cytometry Core for assistance in mass cytometry studies.

Contributors EJS, JA, PS and LF conceptualized the study. LZ, EJS and LF designed the study. SS, JM, EL, KA, AC, SN, CN, TF, RA, EJS and PS collected data. MS, LZ and BC performed statistical data analysis. MS, LZ, BC, MHS and LF interpreted the data. MS, LZ, EJB and LF wrote and edited the manuscript. All authors approved the final version of the article. LF acquired funding for the study. LF supervised the study.

Funding The clinical trial was supported in part by Dendreon and Bristol Myers Squibb (BMS). LF was supported by a Prostate Cancer Foundation Challenge Grant, NCI R01CA223484, U01CA233100, and U01CA244452. MHS was supported by NIH DP50D023056. JA, PS, and SS were supported by Stand Up To Cancer-Cancer Research Institute Cancer Immunology Dream Team Grant SU2CAACR-DT1012 and a Prostate Cancer Foundation Challenge Grant. PS is also supported by Cancer Prevention Research in Texas Grant RP120108, NCI CA1633793, and NCI P30CA016672. SS was also supported by a PCF Young Investigator Award. The UCSF Parnassus Flow Cytometry Core is supported by NIH grant P30 DK063720 and by the NIH Instrumentation Grant S10 1S100D018040-01.

Competing interests SS reports personal fees from Exelixis, Dava Oncology, Cancer Now, Polaris, and MEDACorp; grants and non-financial support from Parker Institute for Cancer Immunotherapy; grants, personal fees, and non-financial support from Janssen Oncology, AstraZeneca, and BMS; personal fees and non-financial support from Dendreon, Amgen, Bayer, and Society for Immunotherapy of Cancer; and personal fees and ownership interests from Apricity Health, unrelated to the work here. TWF reports advisory fees from Med BioGene, AstraZeneca, Foundation Medicine, Janssen, Pfizer, AbbVie, Dendreon, Dava Oncology; research funding from Janssen, Seattle Genetics, Incyte, Bristol Myers Squibb, Neon Therapeutics and Roche/Genentech, unrelated to the work here. PS reports stock options and advisory fees from Oncolytics, Jounce, BioAlta, Forty-Seven, Polaris, Marker Therapeutics, Codiak, ImaginAB, Hummingbird, Dragonfly, Lytix, Lava Therapeutics, Achelois, Infinity, and Glympse, and stock options with BioNTx and Constellation, unrelated to the work here. RA reports research support from Merck, unrelated to the work here. EJS reports advisory fees from Janssen, Fortis, Teon Therapeutics, Ultragenyx, Beigene Consulting, Tolero Consulting; ownership interests in Fortis Therapeutics and Harpoon Therapeutics, unrelated to the work here. LF reports research support from Abbvie, Bavarian Nordic, Bristol Myers Squibb, Dendreon, Janssen, Merck, Roche/Genentech; ownership interests in Actym, Allector, Atreca, BioAlta, Bolt, Keyhole, Immunogenesis, Nutcracker, RAPT, Scribe, Senti, Soteria, and TeneoBio.

Patient consent for publication Not required.

Provenance and peer review Not commissioned; externally peer reviewed.

Data availability statement Data are available upon reasonable request. Mass cytometry data will be shared publicly in a data repository.

Open access This is an open access article distributed in accordance with the Creative Commons Attribution Non Commercial (CC BY-NC 4.0) license, which permits others to distribute, remix, adapt, build upon this work non-commercially, and license their derivative works on different terms, provided the original work is properly cited, appropriate credit is given, any changes made indicated, and the use is non-commercial. See <http://creativecommons.org/licenses/by-nc/4.0/>.

ORCID iD

Meenal Sinha <http://orcid.org/0000-0002-4008-4080>

REFERENCES

- Kantoff PW, Higano CS, Shore ND, *et al*. Sipuleucel-T immunotherapy for castration-resistant prostate cancer. *N Engl J Med* 2010;363:411–22.
- Madan RA, Antonarakis ES, Drake CG, *et al*. Putting the pieces together: completing the mechanism of action jigsaw for Sipuleucel-T. *J Natl Cancer Inst* 2020;112:562–73.



- 3 Fong L, Carroll P, Weinberg V, *et al.* Activated lymphocyte recruitment into the tumor microenvironment following preoperative sipuleucel-T for localized prostate cancer. *J Natl Cancer Inst* 2014;106. doi:10.1093/jnci/dju268. [Epub ahead of print: 24 09 2014].
- 4 Hagihara K, Chan S, Zhang L, *et al.* Neoadjuvant sipuleucel-T induces both Th1 activation and immune regulation in localized prostate cancer. *Oncimmunology* 2019;8:e1486953.
- 5 Beer TM, Kwon ED, Drake CG, *et al.* Randomized, double-blind, phase III trial of ipilimumab versus placebo in asymptomatic or minimally symptomatic patients with metastatic Chemotherapy-Naive castration-resistant prostate cancer. *J Clin Oncol* 2017;35:40–7.
- 6 Kwon ED, Drake CG, Scher HI, *et al.* Ipilimumab versus placebo after radiotherapy in patients with metastatic castration-resistant prostate cancer that had progressed after docetaxel chemotherapy (CA184-043): a multicentre, randomised, double-blind, phase 3 trial. *Lancet Oncol* 2014;15:700–12.
- 7 Fizazi K, Drake CG, Beer TM, *et al.* Final analysis of the ipilimumab versus placebo following radiotherapy phase III trial in Postdocetaxel metastatic castration-resistant prostate cancer identifies an excess of long-term survivors. *Eur Urol* 2020;78:822–30.
- 8 Scher HI, Halabi S, Tannock I, *et al.* Design and end points of clinical trials for patients with progressive prostate cancer and castrate levels of testosterone: recommendations of the prostate cancer clinical trials Working group. *J Clin Oncol* 2008;26:1148–59.
- 9 Sboner A, Karpikov A, Chen G, *et al.* Robust-linear-model normalization to reduce technical variability in functional protein microarrays. *J Proteome Res* 2009;8:5451–64.
- 10 Kotecha N, Krutzik PO, Irish JM. Web-based analysis and publication of flow cytometry experiments. *Curr Protoc Cytom.* 2010;Chapter 10:Unit10 17.
- 11 Levine JH, Simonds EF, Bendall SC, *et al.* Data-Driven phenotypic dissection of AML reveals Progenitor-like cells that correlate with prognosis. *Cell* 2015;162:184–97.
- 12 Spitzer MH, Carmi Y, Reticker-Flynn NE, *et al.* Systemic immunity is required for effective cancer immunotherapy. *Cell* 2017;168:487–502.
- 13 Sheikh NA, Petrylak D, Kantoff PW, *et al.* Sipuleucel-T immune parameters correlate with survival: an analysis of the randomized phase 3 clinical trials in men with castration-resistant prostate cancer. *Cancer Immunol Immunother* 2013;62:137–47.
- 14 Kavanagh B, O'Brien S, Lee D, *et al.* Ctl4 blockade expands Foxp3+ regulatory and activated effector CD4+ T cells in a dose-dependent fashion. *Blood* 2008;112:1175–83.
- 15 Chen H, Liakou CI, Kamat A, *et al.* Anti-Ctla-4 therapy results in higher CD4+ICOShi T cell frequency and IFN-gamma levels in both nonmalignant and malignant prostate tissues. *Proc Natl Acad Sci U S A* 2009;106:2729–34.
- 16 Ng Tang D, Shen Y, Sun J, *et al.* Increased frequency of ICOS+ CD4 T cells as a pharmacodynamic biomarker for anti-CTLA-4 therapy. *Cancer Immunol Res* 2013;1:229–34.
- 17 Slovin SF, Higano CS, Hamid O, *et al.* Ipilimumab alone or in combination with radiotherapy in metastatic castration-resistant prostate cancer: results from an open-label, multicenter phase I/II study. *Ann Oncol* 2013;24:1813–21.
- 18 Cha E, Klinger M, Hou Y, *et al.* Improved survival with T cell clonotype stability after anti-CTLA-4 treatment in cancer patients. *Sci Transl Med* 2014;6:238ra70.
- 19 Rudqvist N-P, Pilonis KA, Lhuillier C, *et al.* Radiotherapy and CTLA-4 blockade shape the TCR repertoire of tumor-infiltrating T cells. *Cancer Immunol Res* 2018;6:139–50.
- 20 Twyman-Saint Victor C, Rech AJ, Maitly A, *et al.* Radiation and dual checkpoint blockade activate non-redundant immune mechanisms in cancer. *Nature* 2015;520:373–7.
- 21 Formenti SC, Rudqvist N-P, Golden E, *et al.* Radiotherapy induces responses of lung cancer to CTLA-4 blockade. *Nat Med* 2018;24:1845–51.
- 22 Postow MA, Callahan MK, Barker CA, *et al.* Immunologic correlates of the abscopal effect in a patient with melanoma. *N Engl J Med* 2012;366:925–31.